ISSN 1330-3651 (Print), ISSN 1848-6339 (Online)
https://doi.org/10.17559/TV-20250414002592
Original scientific paper

Experimental and Numerical Evaluation of Residual Stresses Caused by Welding the Nozzle to the Header

Darko DAMJANOVIC*, Marko PAVKOVIC, Rehan KHAN, Lorenzo SCAPPATIACCI

Abstract: Residual stresses play a critical role in determining the structural integrity and performance of engineering components and systems. This paper presents a comprehensive investigation into the numerical and experimental assessment of residual stresses caused by welding nozzles to the header. The diameter and wall thickness of the nozzle as well as the diameter of the header are the same in all considered cases, while the wall thickness of the header wall is varied. Three specimens were investigated. The research aims to provide a deeper understanding of the influence of header wall thickness to the residual stresses caused by welding. The Finite Element Method was used to model the heat input during welding and evaluate the residual stresses and deformations. The main focus is on the residual stresses. The numerical models are validated against experimental measurements using semi-destructive measurement method: Incremental Hole Drilling Method according to ASTM E837. The data obtained from experiments are compared with the numerical simulations, leading to a comprehensive assessment of the model's accuracy and predictive capabilities. A very good correlation between both, experimental and numerical approach was obtained. In particular, the study demonstrates that increasing the wall thickness of the header leads to higher residual stresses near the weld, which is crucial information for design engineers aiming to balance mechanical strength with stress control. The validated numerical approach also provides a reliable tool for early-stage design optimization, enabling engineers to simulate and refine welding strategies before actual fabrication. The combination of experimental and numerical approaches provides a holistic view of residual stress evaluation and its applications across various industries, specific in this paper, in the boiler industry, where the equipment operates under pressure and elevated temperatures and weld residual stresses should not be neglected as usual.

Keywords: ASTM E837; header; nozzle; residual stress; welding

1 INTRODUCTION

In the domain of structural engineering and materials science, the dependable operation of pressure vessels, pipelines, and various industrial apparatus hinges upon the reliability and integrity of welded components. As a result of welding, a local heat input and subsequent rapid cooling, large residual stresses occur in the weld itself and in its vicinity, and as a consequence, deformation of the structure. These stresses very often reach the yield point of the material and can induce and accelerate its fatigue, brittle or corrosion failure [1, 2]. Deformation that occurs after welding results in dimensional deviations, which is a problem when assembling structures. Subsequent correction of undesirable deformed shapes requires additional time and financial costs. Residual stresses and deformations as a result of welding, as well as ways of minimizing them [3], have been the subject of many studies since the introduction of welding technology into application at the beginning of the nineteenth century. Furthermore, combination of high residual stresses and working load stresses in the weld area can promote fatigue cracking, brittle failure, or corrosion failure. That is why it is important to take residual stresses into account when calculating the structural load-bearing capacity, and when assessing the integrity of a welded component with a crack.

T-joints connecting nozzles to headers, pervasive within such systems, are pivotal points of stress concentrations [4]. Residual stresses within these welded regions wield substantial influence over mechanical performance and fatigue life. Residual stresses are an intrinsic outcome of the welding process, emanating from non-uniform heating and cooling during fabrication [5, 6]. In the context of T-joints, these internal stresses become particularly intricate due to the complex geometries and the diversity of welding parameters involved [7]. Accurate measurement and understanding of residual stresses are crucial for ensuring the long-term reliability of industrial infrastructure and for effectively addressing issues such as fatigue and fracture [8-10].

There are various experimental procedures to measure residual stresses such as for example X-ray diffraction (XRD) [11, 12], neutron diffraction [13], contour method [14] and Incremental Hole Drilling Method (IHDM) [15-17]. In this specific case, IHDM was used as one of the most reliable and the most widely used methods for determining residual stresses. Measurement techniques offer critical data for assessing the real-world stress distribution within T-joints and are instrumental in engineering applications. But when it is necessary to measure the residual stress from welding in a T-joint, the disadvantage of the specific IHDM is that due to size of rosette, it cannot be positioned close enough to the weld, so in addition to other available experimental methods, numerical simulations are quite a necessary approach.

Using the simulation approach to model residual stresses enable the comprehensive analysis of stress distribution within T-joints and their adjacent structures, ultimately contributing to enhanced safety and reliability in industrial systems [18]. This scientific paper is dedicated to the investigation of residual stresses in T-joints connecting nozzles to headers by experimental and numerical approaches. The insights gained from this research aim to augment understanding of residual stress distribution within T-joints, providing a basis for optimizing design and welding processes in pressure vessels and piping systems. By investigating the effects of various geometric configurations in means of wall thickness of header, simulations can offer valuable insights into optimizing welding procedures and mitigating detrimental residual stresses [19-21]. As part of this research, it was shown that even with a modest data regarding welding parameters, a reliable distribution of residual stresses from welding can be obtained by numerical simulation.

2 MATERIALS AND METHODS

Within research conducted in this paper, an experimental approach was used to determine residual stresses from welding in the vicinity of the welded joint between the nozzle and the header. The used experimental method is semi-destructive, called Incremental hole drilling method which is standardized according to ASTM E837 [22]. The numerical modelling of the welding process of the joints was carried out using the classical method, the method of birth and death of elements. The numerical models are validated against experimental measurements.

The material used in this work is boiler steel P235GH-TC2 (EN 10216-2) with further characteristics: density ρ = 7800 kg/m^3, Poisson's ratio ν = 0,3, Young's modulus of elasticity E = 190 GPa, yield strength R_e = 235 MPa and tensile strength R_m = 460 MPa. The thermal properties of the selected material are: thermal conductivity is k = 60,5 W/m°C and specific heat is c_p = 434 J/kg°C. Selected material is very often used in boiler industry.

The diameter and wall thickness of the nozzle as well as the diameter of the header are the same in all considered cases, while the wall thickness of the header is varied. Three specimens were investigated. Fig. 1 shows the considered test specimens with designation of each one as well as weld detail.

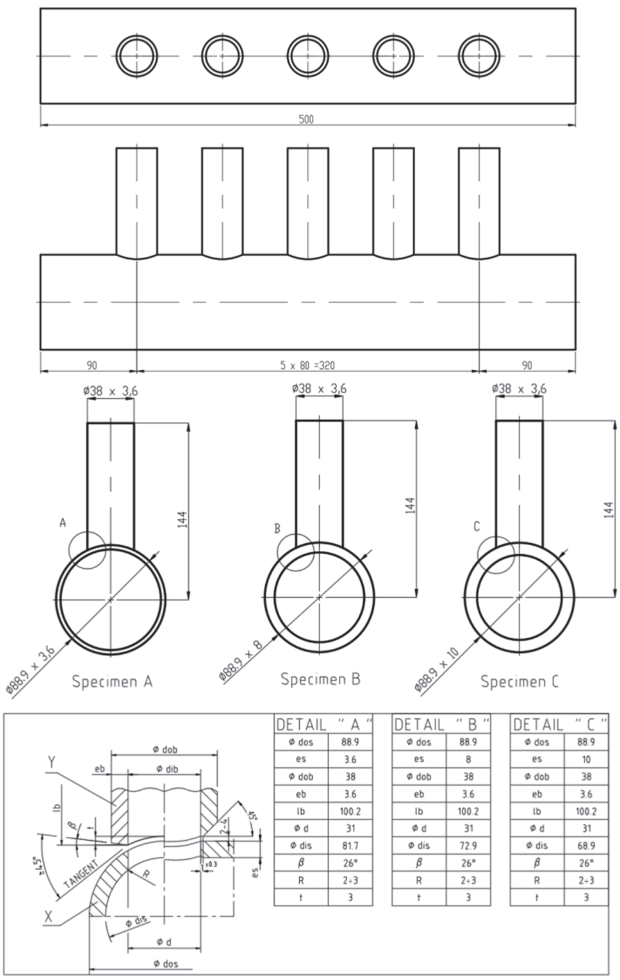

DETAIL "A"		DETAIL "B"		DETAIL "C"	
ϕ dos	88.9	ϕ dos	88.9	ϕ dos	88.9
es	3.6	es	8	es	10
ϕ dob	38	ϕ dob	38	ϕ dob	38
eb	3.6	eb	3.6	eb	3.6
lb	100.2	lb	100.2	lb	100.2
ϕ d	31	ϕ d	31	ϕ d	31
ϕ dis	81.7	ϕ dis	72.9	ϕ dis	68.9
β	26°	β	26°	β	26°
R	2÷3	R	2÷3	R	2÷3
t	3	t	3	t	3

Figure 1 Considered specimens with weld detail

In all three considered specimens, nozzles are welded to the header with two passes using TIG welding method. Fig. 2a shows an example of Specimen B in manufacturing process of welding nozzles to the header, and Fig. 2b shows Specimen B after NDT penetrant testing.

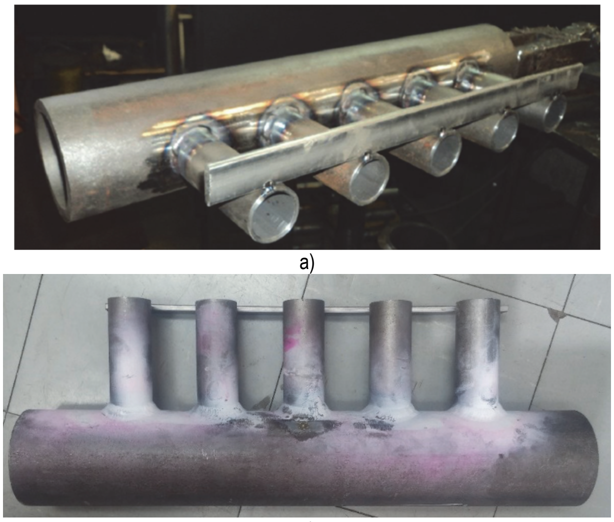

a)

b)

Figure 2 Specimen B: a) during welding nozzles to header, b) after NDT penetrant testing

Heat input is calculated hereafter on example of Specimen A. Parameters of TIG welding:
Current strength of TIG welding: I = 220A.
TIG welding voltage: U =14 V.
The degree of beneficial effect of TIG welding: η = 0,6.
Calculation of welding power at given parameters:

$$Q = U \times I \times \eta = 220 \times 14 \times 0,6 = 1848 \text{ W} \quad (1)$$

Volume of one weld segment:

$$V = \frac{z^2}{2} \times L = \frac{4^2}{2} \times 7,46 = 59,7 \text{ mm}^3 \quad (2)$$

Where:
z - weld cathetus /mm
L - length of one weld segment /mm

Internal heat generation in one weld segment [21]:

$$q_V = \frac{Q}{V} = \frac{1848}{59,7} \approx 31 \text{ W/mm}^3 \quad (3)$$

2.1 Incremental Hole Drilling Method (IHDM)

The IHDM is categorized as a semi-destructive method and is widely used for relatively inexpensive and reliable determination of residual stresses. For the research in this paper, RESTAN MTS3000 is used for measuring residual stresses. The flat end mill 1-SINTCTT/1 with a diameter of 1,8 mm is used to drill hole to a depth of 1 mm in 10 steps with polynomial interpolation between each drilling step.

Strain gauge rosette type HBM-1.5/120RY61S with strain gauges positioned at 0°/45°/90° is used to measure the strains on the surface of the samples. The measurement is performed on each specimen at the same location (at the middle nozzle, distance from weld toe to the center of strain gauge rosette is 6 mm). Measurements were made in the laboratory at room temperature. Fig. 3 shows the basic steps in residual stress measurement using IHDM: a) preparing the surface, b) positioning strain gauge rosette, c) wiring the strain gauge rosette, d) positioning the hole drilling device and e) drilling the hole.

a)

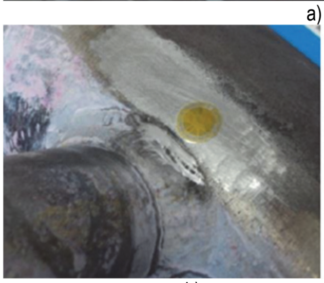

b)

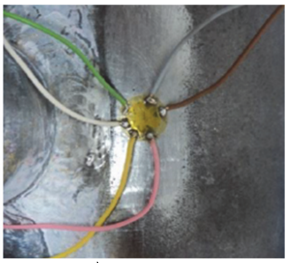

c)

d)

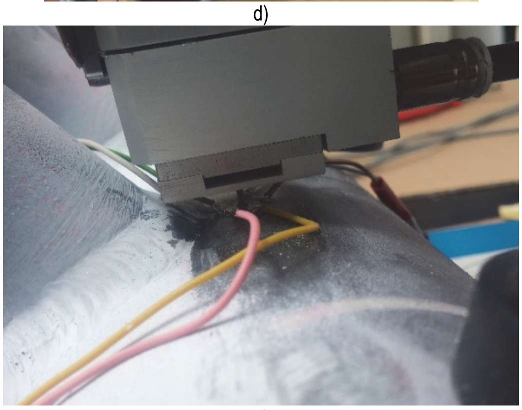

e)

Figure 3 Example of measuring residual stresses using IHDM on Specimen B a) preparing the surface, b) positioning strain gauge rosette, c) wiring strain gauge rosette, d) positioning the hole drilling device, e) drilling the hole

The surface was sanded and polished, and then adequately cleaned and degreased with medicinal alcohol. The rosette is positioned in such a way that the measuring tape in the rosette marked "c" is placed in the circumferential direction of the header, Fig. 4. Rosette is glued with HBM Z70 glue, and wired with Spider 8 amplifier.

Fig. 4 shows orientation of strain gauge rosette in each measurement. Strain gauge rosette is orientated in the way that strain gauge "a" within the rosette is directed in longitudinal direction of header, strain gauge "c" within the rosette is directed in circumferential direction of header and strain gauge "b" within strain gauge rosette is directed perpendicular to "a", Fig. 4. The outcome results of measurement are principal stresses σ_1, σ_2 and orientation of principal coordinate system in means of angle β, Fig. 4.

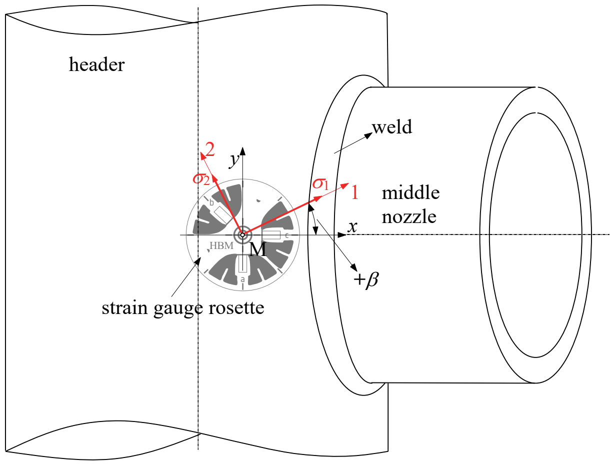

Figure 4 Orientation of strain gauge rosette in vicinity of weld at the middle nozzle

While IHDM is widely recognized as a reliable and cost-effective technique for measuring residual stresses, it does have several limitations with particular use like in this paper. Due to the physical size of the strain gauge rosette, it cannot be positioned very close to the weld toe. This restricts the ability to capture the highest stress gradients, which typically occur near the weld.

In this particular case, strain gauge rosette is placed as much as close to the weld toe which gives distance from the weld toe to center of rosette of 6 mm.

2.2 Numerical Analysis of Residual Stresses

The numerical analysis of the welding process has a significant influence on the selection of finite elements, modelling of heat input and selection of weld material and base material. For the most realistic modelling of heat input and the most accurate assessment of residual stresses and deformations, it is necessary to carry out the simulation using a three-dimensional (3D) model and the element birth and death technique [23]. One of the problems in the simulation of the welding process is that it is necessary to know the thermal and mechanical properties of the material at elevated temperatures, up to the melting temperature. These data significantly affect the result.

In this specific work, the transient thermal (for temperature calculation) and transient structural (calculation of residual stresses as a result of excessive heating and deformation) calculations were used.

When conducting this kind of numerical analysis, it is necessary to know how much each segment of the weld is heated in a certain time.

Tab. 1 shows the results for Internal heat generation for each considered specimen, which were obtained by the mentioned calculation. It was obtained in this way due to modest data regarding welding parameters.

Table 1 Calculated values of internal heat generation for each considered specimen

Specimen designation	Header thickness t / mm	Number of welding passes	Internal heat generation q_v / W/mm^3
Specimen A	3,6	2	31
Specimen B	8	2	32
Specimen C	10	2	36

The 3D model was constructed such that the first and second welding passes were modelled separately and divided into smaller volumes to enable time-dependent heat allocation during the simulation. The total simulation time was 400 seconds, of which 32 seconds were dedicated to welding (16 seconds per pass), followed by 368 seconds of cooling. No intermediate cooling phase was introduced between the two passes, which is a simplification compared to real-world welding procedures. Each pass was discretized into 16 elements, implying a time step of approximately 1 second per element. Although welding speed was not explicitly defined, the element size and time step were selected to reflect a realistic progression of the heat source. The welding parameters: current, voltage and efficiency were assumed constant for both passes, resulting in a uniform heat input of 1848 W. This assumption, along with the omission of inter-pass cooling and potential thermal interactions between passes, is acknowledged as a limitation of the model. On one end of the header, displacements were restricted in all directions, while on the opposite end, displacement was allowed in the longitudinal direction but restricted radially. These boundary conditions were applied to simulate realistic mechanical constraints during welding.

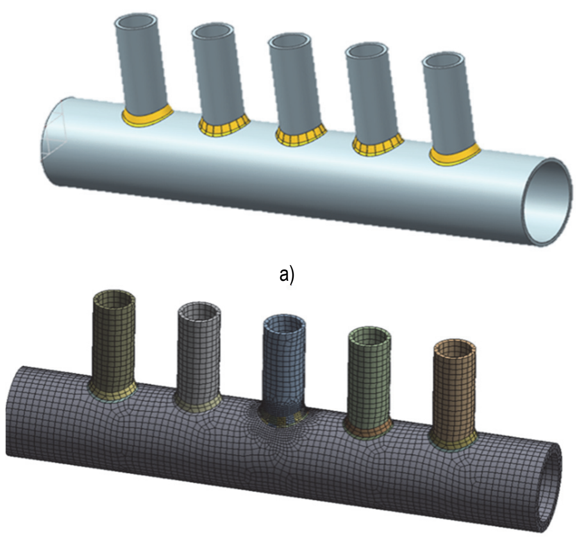

a)

b)

Figure 5 Orientation of strain gauge rosette in vicinity of weld at the middle nozzle

The material is modelled as elastic-ideally plastic, since the influence of material hardening on the amount of residual stresses is negligible in low-carbon steels [24].

Finite element mesh was generated with hexahedral finite elements in the way that global size of the finite element is 6 mm, while 2 mm finite element size was generated locally in the weld area of the middle nozzle. Fig. 5a shows an example of 3D model with generated welds which are separated into smaller volumes and Fig. 5b shows corresponding finite element mesh.

While the numerical model used in this study provides valuable insights into residual stress distribution due to welding, several limitations should be acknowledged. The simulation assumes that all weld volumes and passes are already present in the model, and only heat input is applied sequentially. This approach does not fully capture the real-time evolution of the weld, where each pass affects the thermal and mechanical response of the subsequent ones. Further, the model simulates welding of only the middle nozzle, whereas in the experimental setup, five nozzles are welded. The thermal and mechanical interactions between adjacent welds are not considered, which can significantly influence the residual stress field. For future work, the authors aim to enhance the simulation by implementing more advanced techniques that simulate the actual deposition of weld material over time, allowing for more realistic thermal and mechanical interactions. Additionally, the influence of neighbouring nozzles will be incorporated into the model to better capture the stress field in multi-nozzle configurations. Further improvements will also include modelling variable heat input between passes, introducing inter-pass cooling phases, and refining the relationship between welding speed, element size, and time step. These enhancements are expected to significantly improve the physical accuracy and predictive capability of the numerical model.

3 RESULTS AND DISCUSSION

Outputs of experimental measurement using the Incremental Hole Drilling Method are deformations in the direction of each strain gauge within strain gauge rosette ε_a, ε_b, ε_c, orientation of principal coordinate system β, principal stresses σ_1 and σ_2 as well as corresponding equivalent stresses according to the Von Mises and Tresca criteria. Tab. 2, Tab. 3 and Tab. 4 show values for β, σ_1, σ_2 as well as equivalent stresses according to the Von Mises and Tresca criteria for each considered specimen. Fig. 6, Fig. 7 and Fig. 8 show diagrams for principal stresses and angles β for each considered specimen up to a depth of measurement 1 mm.

Table 2 Measured values for Specimen A

Depth / mm	β / °	σ_2 / MPa	σ_1 / MPa	Von Mises / MPa	Tresca / MPa
0,05	−81,23	−84,23	2,042	85,153	86,156
0,149	−84,07	22,52	149,53	139,63	149,53
0,248	82,73	33,61	234,88	220,012	234,88
0,347	74,07	45,2	278,63	259,002	278,63
0,446	69,97	49,34	281,96	260,816	281,96
0,546	68,28	48,33	271,08	250,44	271,08
0,645	67,75	61,64	286,76	261,443	286,76
0,744	67,78	78,82	306,35	275,525	306,35
0,843	68,14	68,56	274,22	247,177	274,22
0,943	68,76	63,035	282,87	257,209	282,87

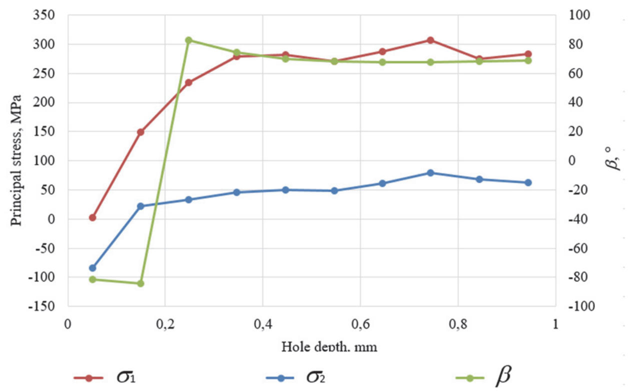

Figure 6 Principal stresses and angle of principal coordinate system versus measurement depth Specimen A

Table 3 Measured values for Specimen B

Depth/ mm	β / °	σ_2 / MPa	σ_1 / MPa	Von Mises /MPa	Tresca /MPa
0,05	−13,61	−95,71	43,313	123,218	139,027
0,149	−4,728	−98,68	210,42	273,457	309,1
0,248	−2,745	−75,87	233,587	279,355	309,451
0,347	−1,813	−63	219,898	257,251	282,899
0,446	−1,116	−53,09	226,053	256,748	279,142
0,546	−0,616	−42,03	236,78	260,35	278,807
0,645	−0,277	−29,61	231,48	247,618	261,093
0,744	0,006	−14,78	222,921	230,663	237,694
0,843	0,235	−3,275	231,713	233,368	234,988
0,943	0,311	−17,78	211,451	220,88	229,234

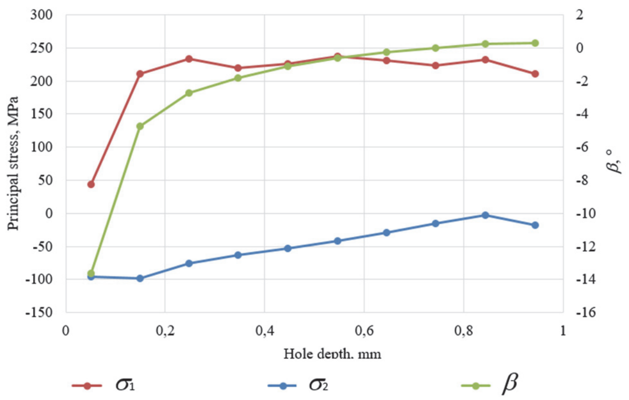

Figure 7 Principal stresses and angle of principal coordinate system versus measurement depth Specimen B

Table 4 Measured values for Specimen C

Depth/ mm	φ / °	σ_2 / MPa	σ_1 / MPa	Von Mises /MPa	Tresca /MPa
0,05	15,74	−159,3	−3,012	157,829	159,314
0,149	5,218	−175,1	125,851	261,793	300,952
0,248	4,393	−166,1	133,201	259,701	299,276
0,347	5,157	−161,7	133,202	255,757	294,865
0,446	6,227	−154,1	141,199	255,774	295,249
0,546	7,222	−139,7	149,167	250,169	288,818
0,645	8,041	−123,2	155,019	241,435	278,178
0,744	8,715	−108,9	157,959	232,449	266,913
0,843	9,325	−103,3	153,915	224,229	257,266
0,943	9,93	−118,3	136,64	221,007	254,978

Fig. 9 shows comparison of experimental results in the means of Von Mises stress for each specimen up to depth of 1 mm.

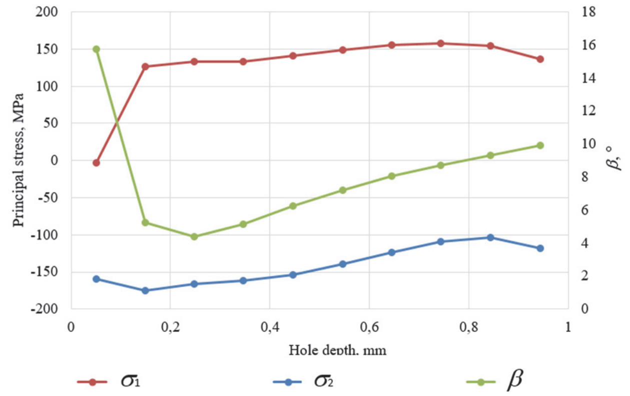

Figure 8 Principal stresses and angle of principal coordinate system versus measurement depth Specimen C

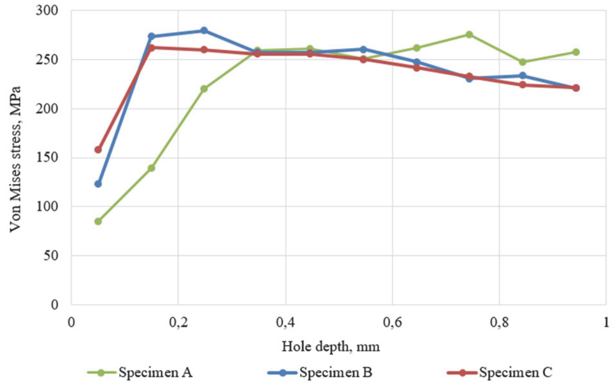

Figure 9 Von Mises stress for each specimen up to depth of 1 mm

A very similar trend of Von Mises stress for each considered specimen is obvious from Fig. 9. In fact, from 0,35 to 0,6 of measurement depth, there are practically very similar measured values of Von Mises stress.

Regarding numerical simulations, results are shown for each considered specimen in means of temperatures after 400 seconds of simulation and residual stresses around the middle nozzle as well as detail of residual stresses distribution in the area where the strain gauge rosette is placed in experimental measurements. Fig. 10 shows temperature distribution for all three specimens after 400 seconds.

It is obvious from Fig. 10 there is very similar temperature distribution in all three cases where the middle nozzle is cooled last. The average temperature in the weld zone is around 40 - 60 °C in all three cases.

Fig. 11 shows residual stress distribution (Von Mises) after 400 s for all three considered specimens.

The right hand side of Fig. 11 shows areas where the strain gauge rosette is positioned in the experimental measurements. Those values are taken into account for calculating mean value of Von Mises equivalent stress for each specimen. It should be noted here that in the case of experimentally obtained results, for the purpose of comparison, mean value of Von Mises stress is calculated from 0,25 mm to 0,85 mm of depth. The area from 0 to 0,25 mm of depth as well as the area from 0,85 to 1 mm of depth is the area where is possible uncertainty present in measurements, and thus, unreliable results. Area from 0 to 0,25 mm is the area that should not be taken into account when measuring on curved surfaces.

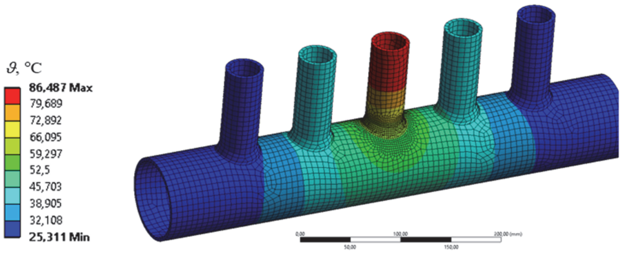

a)

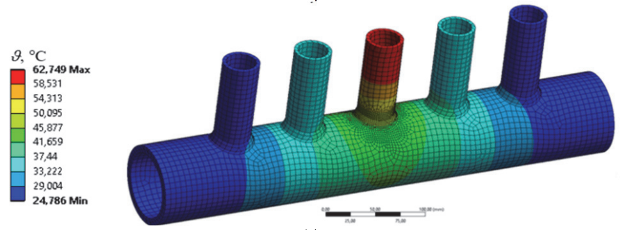

b)

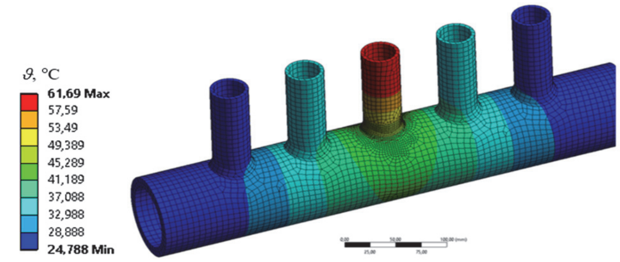

c)

Figure 10 Temperature distribution after 400 s:
a) Specimen A, b) Specimen B, c) Specimen C

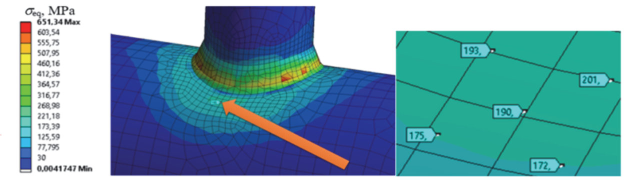

a)

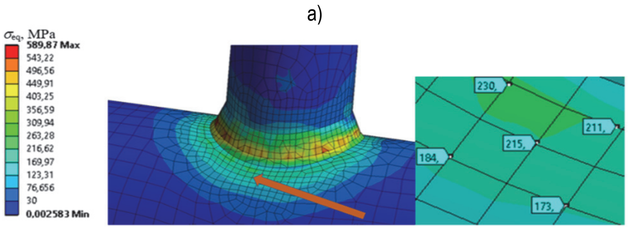

b)

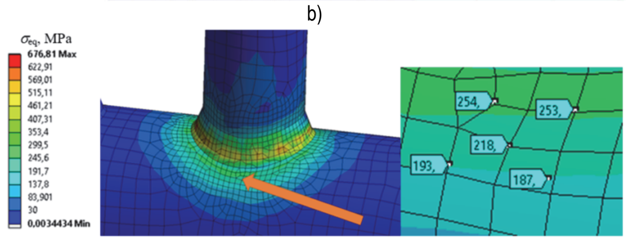

c)

Figure 11 Residual stress distribution (Von Mises):
a) Specimen A, b) Specimen B, c) Specimen C

Further, surface preparation as well as uncertainty of positioning cutter to the zero position can affect the results [25]. In this specific case, residual stresses are measured on hot-rolled pipes, due to the technology of production of this kind of pipes, high gradients of deformations can occur near the surface of a pipe. Further, the area from 0,85 to 1 mm is recommended not to be taken into account, because of radius of cutter (so, a small radius is present in the hole in the final measurement step, which can affect the measurement results) [25]. Taking into account all mentioned, the area of relevant values from which the mean Von Mises stress is calculated is taken into account from 0,25 mm to 0,85 mm of depth. A comparison of the results shows a very good correlation between the experimental and numerical results. Fig. 12 shows the comparison of Von Mises mean values obtained from numerical simulations versus Von Mises stresses obtained from experimental measurements.

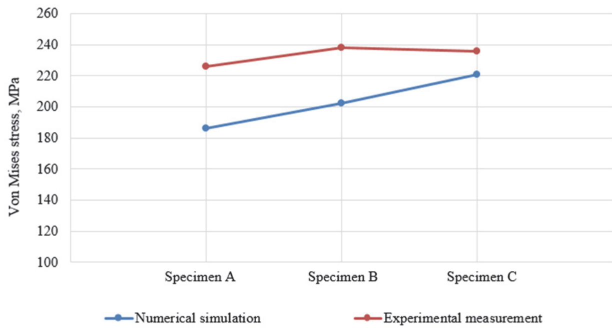

Figure 12 Comparison of numerical and experimental results of Von Mises equivalent stress

A very similar trend of Von Mises stress is obvious for both, experimental and numerical results. Some deviations in results are expected due to a lot of factors. First of all, in numerical simulations, welding of only middle nozzle is simulated, and in experimental specimens, all five nozzles are welded. Besides welding the middle nozzle, neighbor nozzles also contribute to the residual stresses at the measurement point in the vicinity of weld in the middle nozzle. Further, residual stresses in pipes as such are presented in real pipes due to production process, but those residual stresses are not taken into account in numerical simulations. In fact, residual stresses in pipes, which are the result of production process, can be significant [15].

Numerical simulations conducted within this research are conducted in the way that all weld volumes and passes are already present in the model through simulation, so only the heat is generated in each one separately (at a certain time). Because of this, such a method is unrealistic, because the previous element affects the next one, which in reality has not even appeared yet. Taking into account all the mentioned facts it is expected that stresses obtained by numerical simulations would be smaller than the residual stresses obtained by experimental measurements on real specimens.

4 CONCLUSIONS

Within this research, three specimens are analyzed experimentally and numerically. Specimens represent header-nozzle connection where the dimensions of the nozzle in the case of diameter and wall thickness are the same in all three specimens. In the header, the diameter is constant for all three specimens while wall thickness is varied. In all three specimens, nozzles are welded to the header by two passes each.

By comparing numerical and experimental results, a very similar trend of both is obtained. But it is expected that by analyzing exact values of residual stresses there should be some deviations. Deviations are expected due to a lot of factors. In the experimental part, all five nozzles are welded to the header. So all five nozzles, i.e. welding of all five nozzles, contribute to residual stresses at the vicinity of the weld at the middle nozzle where residual stresses are measured. In numerical simulation, only welding of the middle nozzle is simulated. It is very important to note here also that in numerical simulations, residual stresses that are present in pipes themselves, are not simulated. Those residual stresses are the results of production process of hot-rolled pipes which includes hot rolling, sizing and straightening in several stages. Besides that, it includes heating of material to high temperatures and after production process, uneven cooling can occur. All the mentioned affects the residual stresses in pipes after the production process. Again, residual stresses which are the result of production process are not taken into account in numerical simulations conducted in this research. Further, the character of residual stresses can be very unexpected, i.e. residual stresses can be very different for two measurement points on the same specimen.

Regarding numerical simulations conducted within this research, it is important to note here that weld volumes and passes are already present in the model through simulation, so only the heat is generated in each weld volume separately. So this method is unrealistic, because the previous element affects the next one, which in reality has not even appeared yet.

By taking into account all the mentioned facts it is expected that simulated stresses would be smaller than the measured ones. In general, when taking into account all mentioned factors and character of residual stresses themselves, a very good correlation between experimental and numerical results is obtained and this method of simulating residual stresses can be used in some early stages for optimizing weld parameters between components.

In further work, it is planned to simulate the welding process on both neighboring nozzles as well because heat input on neighboring nozzles also affects the middle nozzle, so the assumption is that numerical results will be even closer to the experimental results. Further, the plan is to make simulation more real, meaning that when the heat input is generated in the weld volume, in that specific moment, the volume itself appears. In this way, the influence of the heat input on the not yet generated weld volumes will be avoided, which is more realistic than current simulations conducted within this research.

Acknowledgements

The authors would like to acknowledge the EU Research Project (NPOO.C3.2. R3-I1.04.0117) financed from The Recovery and Resilience Facility (NextGenerationEU).

5 REFERENCES

[1] Chiocca, F., Frendo, F., Aiello, F., & Bertini, L. (2022). Influence of residual stresses on the fatigue life of welded joints: Numerical simulation and experimental tests. *International Journal of Fatigue, 162*. 106984. https://doi.org/10.1016/j.ijfatigue.2022.106901

[2] Szavai, S., Kovacs, S., Bezi, Z., & Kozak, D. (2021). Coupled numerical method for rolling contact fatigue analysis. *Technical Gazette, 28*(5), 1560-1567. https://doi.org/10.17559/TV-20201117124940

[3] Radaj, D. (1992). Reduction of welding residual stresses and distortion. *Heat Effects of Welding, Temperature Field, Residual Stress, Distortion,* 247-313. https://doi.org/10.1007/978-3-642-48640-1_4

[4] Hectors, K. & De Waele, W. (2021). Influence of weld geometry on stress concentration factor distributions in tubular joints. *Journal of Constructional Steel Research, 176*, 106412. https://doi.org/10.1016/j.jcsr.2021.106412

[5] Fitzpatrick, M. E. & Lodini, A. (2003). *Analysis of residual stress by diffraction using neutron and synchrotron radiation*. Taylor & Francis.

[6] Wang, Y., Guangjie, F., Pu, X., & Deng, D. (2021). Influence of welding sequence on residual stress distribution and deformation in Q345 steel H-section butt-welded joint. *Journal of Materials Research and Technology, 13*, 144-153. https://doi.org/10.1016/j.jmrt.2021.04.059

[7] Jang, G. C., Chang, K. H., & Lee, C. H. (2007). Characteristics of the residual stress distribution in welded tubular T-joints. *Journal of Mechanical Science and Technology, 21*, 1714-1719. https://doi.org/10.1007/BF03177399

[8] Withers, P. J. & Bhadeshia, H. K. D. H. (2001). Residual stress. Part 1 - Measurement techniques. *Materials Science and Technology, 17*(4), 355-365. https://doi.org/10.1179/026708301101509980

[9] James, M. N., Hattingh, D. G., Asquith, D., Newby, M., & Doubell, P. (2016). Applications of residual stress in combatting fatigue and fracture. *Procedia Structural Integrity, 2*, 11-25. https://doi.org/10.1016/j.prostr.2016.06.003

[10] Wang, D., Zhang, H., Gong, B., & Deng, C. (2016). Residual stress effects on fatigue behaviour of welded T-joint: A finite fracture mechanics approach. *Materials & Design, 91*, 211-217. https://doi.org/10.1016/j.matdes.2015.11.106

[11] Varga, G. & Ferencsik, V. (2022). Investigation of the effect of surface burnishing on stress condition and hardening phenomena. *Technical Gazette, 29*(4), 1247-1253. https://doi.org/10.17559/TV-20211110171854

[12] Nowak, W. J., Ochal, K., Filip, R., & Wierzba, B. (2021). The analysis of the residual stress evolution during cycling oxidation of the Ni-base superalloys at high temperature. *Technical Gazette, 28*, 540-547. https://doi.org/10.17559/TV-20200108155228

[13] Harati, E., Karlsson, L., Svensson, L. E., Pirling, T., & Dalaei, K. (2017). Neutron diffraction evaluation of near surface residual stresses at welds in 1300 MPa yield strength steel. *Materials, 10*(6), 593. https://doi.org/10.3390/ma10060593

[14] Wang, H., Dong-Kyu, K., Wanchuck, W., Shi-Hoon, C., Yeol, S. L., & Kwang Hwang, S. (2020). A new contour method for rapid evaluation of the cross-sectional residual stress distribution in complex geometries using a 3D scanner. *Journal of Mechanical Science and Technology, 34*, 1989-1996. https://doi.org/10.1007/s12206-020-0420-0

[15] Damjanović, D., Kozak, D., Marsoner, S., & Gubeljak, N. (2017). Residual stress state in pipe cut ring specimens for fracture toughness testing. *Materialpruefung/Materials Testing, 59*(6), 530-535. https://doi.org/10.3139/120.111038

[16] Damjanović, D., Kozak, D., & Gubeljak, N. (2019). The influence of residual stresses on fracture behavior of Pipe Ring Notched Bend specimen (PRNB). *Engineering Fracture Mechanics, 205*, 347-358. https://doi.org/10.1016/j.engfracmech.2018.10.016

[17] Milkovic, M., Vuherer, T., & Gubeljak, N. (2019). Comparison of two methods for measuring residual stresses in weldments. *Structural Integrity and Life, 19*(2), 125-130.

[18] Acevedo, M., Drezet, J.-M., & Nussbaumer, A. (2012). Numerical modelling and experimental investigation on welding. *Fatigue & Fracture of Engineering Materials & Structures, 36*(2), 177-185. https://doi.org/10.1111/j.1460-2695.2012.01712.x
[19] Zhao, W., Jiang, W., Zhang, H., Han, B., Jin, H., & Gao, Q. (2021). 3D finite element analysis and optimization of welding residual stress in the girth joints of X80 steel pipeline. *Journal of Manufacturing Processes, 66*, 166-178. https://doi.org/10.1016/j.jmapro.2021.04.009
[20] Amirsalari, A. & Golabi, S. (2022). Finite element analysis, prediction, and optimization of residual stresses in multi-pass arc welding with experimental evaluation. *The Journal of Strain Analysis for Engineering Design, 57*(4), 202-214. https://doi.org/10.1177/03093247221078637
[21] ASTM International. (2008). *ASTM E837-08: Standard test method for determining residual stresses by hole-drilling strain-gage method*. ASTM International.
[22] Kovacev, Z., Konjatic, P., Damjanovic, D., & Turk, D. (2021). Welding simulations using element birth and death technique in Ansys and residual stress comparison. In *10th International Scientific-Professional Conference SBW 2019: Engineering Technologies in Manufacturing of Welded Constructions and Products* (SBW 2019), Slavonski Brod.
[23] Mollicone, P., Camilleri, D., Gray, T. G., & Comlekci, T. (2006). Simple thermo-elastic-plastic models for welding distortion simulation. *Journal of Materials Processing Technology, 176*(1-3), 77-86. https://doi.org/10.1016/j.jmatprotec.2006.02.022
[24] Scafidi, L., Valentini, E., & Zuccarello, B. (2011). Error and uncertainty analysis of the residual stresses computed by using the hole drilling method. *Strain, 47*(s2), 301-312. https://doi.org/10.1111/j.1475-1305.2009.00688.x

Contact information:

Darko DAMJANOVIC, Assoc. prof.
(Corresponding author)
University of Slavonski Brod, MEF,
Trg Ivane Brlic Mazuranic 2, 35 000 Slavonski Brod, Croatia
E-mail: ddamjanovic@unisb.hr

Marko PAVKOVIC, MSc. Eng.
Koncar - Metalnekonstrukcije d.o.o.,
Fallerovosetaliste 22, 10 000 Zagreb, Croatia
E-mail: pavkovic.marko2m@gmail.com

Rehan KHAN, PhD
National University of Sciences and Technology,
Islamabad 44000, Pakistan
E-mail: mrehan.khan@ceme.nust.edu.pk

Lorenzo SCAPPATIACCI, PhD
5Allimep SRL,
Via dell' Acciaio 7, 06134 Perugia, Italy
E-mail: scappaticci@allimep.com